Sequential and simultaneous emission of particles from p + Al collisions at GeV energies

M. Fidelus,[1] D. Filges,[2,3] F. Goldenbaum,[2,3] H. Hodde,[4] A. Jany,[1] L. Jarczyk,[1] B. Kamys,[1,*] M. Kistryn,[5] St. Kistryn,[1] St. Kliczewski,[5] E. Kozik,[5] P. Kulessa,[5] H. Machner,[6] A. Magiera,[1] B. Piskor-Ignatowicz,[1,2,3] K. Pysz,[5] Z. Rudy,[1] Sushil K. Sharma,[1,2,3] R. Siudak,[5] and M. Wojciechowski[1]
(PISA Collaboration)
[1]*M. Smoluchowski Institute of Physics, Jagiellonian University, Reymonta 4, 30059 Kraków, Poland*
[2]*Jülich Center for Hadron Physics, Forschungszentrum Jülich, 52425 Jülich, Germany*
[3]*Institut für Kernphysik, Forschungszentrum Jülich, 52425 Jülich, Germany*
[4]*Institut für Strahlen- und Kernphysik, Bonn University, 53121 Bonn, Germany*
[5]*H. Niewodniczański Institute of Nuclear Physics PAN, Radzikowskiego 152, 31342 Kraków, Poland*
[6]*Universität Duisburg-Essen, Fakultät für Physik, Lotharstraße 1, 47048 Duisburg, Germany*
(Received 1 July 2013; revised manuscript received 13 April 2014; published 29 May 2014)

The energy and angular dependence of double differential cross sections $d^2\sigma/d\Omega\, dE$ were measured for p, d, t, ^{3,4,6}He, ^{6,7,8,9}Li, ^{7,9,10}Be, and ^{10,11}B produced in collisions of 1.2, 1.9, and 2.5 GeV protons with an Al target. It was found that the cross sections are almost independent of the beam energy. The spectra and angular distributions indicate a presence of two contributions: a quasi-isotropic, low-energy one which is attributed to the emission of particles from excited remnants of the intranuclear cascade, and an anisotropic part which is interpreted to originate from the first stage of the reaction. The experimental data are compared with an intranuclear cascade model coupled to evaporation, and to statistical multifragmentation models using their standard parameter settings. It was found that all applied models produce very similar results describing spectra of the intermediate mass fragments. All models also reproduce well the low-energy part of the spectra of light charged particles (below $\approx$ 30 MeV). The description of the higher energy part (50–150 MeV) of the light charged particles spectra is poorer, deteriorating with decreasing scattering angle and decreasing mass of the particles.

DOI: 10.1103/PhysRevC.89.054617 PACS number(s): 25.40.Sc, 25.40.Ve

I. INTRODUCTION

In recent studies of reactions induced by GeV protons on Au [1,2] and Ni targets [3,4], it has been found that the inclusive spectra of light charged particles (LCP), i.e., spectra of p, d, t, and α particles, contain two components which differ in energy and angular dependences. The low-energy component of the spectra is almost angle independent, while the high-energy part of the spectra changes with the angle. These tails of the spectra are very distinct and elongated to high energies at small emission angles, but they decrease with increasing angle. A similar, but less pronounced effect was observed in spectra of intermediate mass fragments (IMFs), i.e., particles with $Z \geqslant 3$, but lighter than fission fragments, e.g., Li, Be, B, etc. These properties of the spectra could not be reproduced quantitatively by the traditional two-step model, which assumes that the first stage of the reaction proceeds via an intranuclear cascade of nucleon-nucleon and nucleon-pion collisions, leaving the equilibrated hot nucleus emitting, in the subsequent stage, nucleons and composite particles.

The same effect of the presence of two components in the spectra has been observed for various target nuclei by other authors, e.g., by Green *et al.* [5,6] for reactions in the p + Ag system at $T_p = 0.21$, 0.3, and 0.48 GeV; by Herbach*et al.* [7] for target nuclei between Al and Th at 1.2 GeV; by Letourneau *et al.* [8] for p + Au collisions at 2.5 GeV; by Westfall *et al.* [9] for C, Al, Ag, and U targets irradiated by protons of 2.1 and 4.9 GeV energies; by Hyde *et al.* [10] for the p + Ag system at 5.5 GeV; and by Poskanzer *et al.* [11] for p + U reactions at 5.5 GeV.

The analysis of the energy and angular dependences of differential cross sections for IMFs from p + Au and p + Ni reactions [1–4] has shown that the data can be well reproduced by a phenomenological model that assumes that the composite particles are emitted isotropically from two sources moving along the beam direction. While for the heavier systems (Au, Ni) we focused on the phenomenological description of the reaction mechanism as mentioned above, in the current paper we use a different approach in investigating the p + Al system at GeV energies: The experimental double differential cross sections $d^2\sigma/d\Omega\, dE$ for all ejectiles (p, d, t, ^{3,4,6}He, ^{6,7,8}Li, ^{7,9,10}Be, and ^{10,11}B) are compared to model calculations using an intranuclear cascade code to describe the first fast stage, and to evaporation or statistical multifragmentation codes to account for the second phase of the reaction. The models chosen for the comparison have been selected according to the favored choice of models resulting from a benchmark study for model and code comparisons under auspices of the International Atomic Energy Agency (IAEA) [12,13]. Taking the energy domain of the studied system and applicability of models into account, the proposed choice was therefore including the latest versions of the intranuclear cascade model INCL4.6 [14], the evaporation code ABLA07 [15], the statistical multifragmentation code SMM [16] and GEMINI++ [17,18] which describes the decay of excited

*Corresponding author: ufkamys@cyf-kr.edu.pl

nuclei by a series of binary decays. The primary goal of the comparison to the model calculations is to validate the implemented reaction mechanisms in the codes and test their capability of reproducing the experimental data. Here it is of particular importance to measure double differential cross sections $d^2\sigma/d\Omega\, dE$ rather than total cross sections only, thus imposing additional constraints on the theoretical models and on understanding the complex reaction mechanism itself. Furthermore, the aim is to determine whether the composite particles are predominantly emitted from an equilibrated nucleus, or during the fast intranuclear cascade phase via a coalescence mechanism.

The p + Al system has been selected to compare the double differential cross sections $d^2\sigma/d\Omega\, dE$ for a light target with the data for significantly heavier Au and Ni targets, measured previously [1–4]. The comparison of data obtained at the same experimental conditions can show whether the properties of the spectra and angular distributions remain the same in the full range of target masses. Similarity of the data for all targets may indicate that the same mechanism is responsible for the observed features of the cross sections.

It should be noted that the choice of the Al target extends the previous studies to a very light nucleus which is, however, still heavy enough to preserve the necessary conditions of using the intranuclear cascade models. These models, which neglect the shell structure of nuclei, are known not to work well for very light nuclei (cf., e.g., Fraenkel *et al.* [19]).

The paper is organized as follows: the experimental details are discussed in the next section, the third section is devoted to a brief introduction of the main features of the applied models and to theoretical analysis of the data, whereas the last section summarizes the obtained results and conclusions.

II. EXPERIMENTAL RESULTS

The PISA experiment has been performed using the internal beam of COSY (cooler synchrotron) of the Research Center in Jülich. The apparatus and experimental procedure have been described in previous publications [1,2,4], thus we present here only details concerning the detectors. Double differential cross sections $d^2\sigma/d\Omega\, dE$ were measured at seven scattering angles: 15.6°, 20°, 35°, 50°, 65°, 80°, and 100°. The mass and charge identification of detected particles was realized by the ΔE-E method using telescopes consisting of silicon semiconductor detectors backed for four angles by a 7 cm thick CsI detector with a photo-diode readout, which were used to detect high-energy light charged particles (LCPs) passing through the silicon detectors. The telescopes at three smaller angles (15.6°, 20°, and 65°) were installed in air, behind 50 μm stainless steel foils closing the vacuum of the scattering chamber. The silicon detectors of the telescope at 100° were placed inside the vacuum chamber, whereas the scintillator detector was installed in air. The thicknesses of all detectors are given in Table I.

The energy calibration of the signals from the silicon detectors was achieved by fitting two-dimensional spectra ΔE-E for all pairs of the silicon detectors, taking into account known thicknesses of the detectors and the energy dependence of the energy losses dE/dx in the silicon. For the scintillator detectors where the light output is a nonlinear function of the energy the light output, $L(E,A,Z)$ was parametrized according to Ref. [20] as follows:

$$L(E,A,Z) = a_0 + a_1\{E - a_3 AZ^2 \ln[E/(a_2 AZ^2) + 1]\}.$$

The parameters a_0 and a_1 were fixed at values specific for individual detectors, since they were determined by the electronics setting. The parameters a_2 and a_3, which contain information on quenching of the light signal in CsI, were common for all scintillating detectors. The parameters were fitted to two-dimensional ΔE-E spectra where the information on ΔE was obtained from the silicon detectors placed in front of the scintillator detector, which in turn supplied information on the total E deposit. Of course, the losses of the particle energies in the stainless steel foils were taken into account. The best results of fits were obtained for $a_2 = 75$ MeV, common for all particles, and a_3 equal to 157.5, 150, and 135 MeV for protons, deuterons and tritons, and He ions, respectively.

TABLE I. Laboratory polar angles and thicknesses of the detectors in the ΔE-E telescopes. Thicknesses of the stainless steel foils as well as thicknesses of the silicon detectors are given in μm, those of CsI scintillators in cm.

Angle	Foil		Silicon detectors			Foil	CsI
15.6°	50	89	1016	1016	89		7
20°	50	89	1016	1016	89		7
35°		48	426	6000			
50°		41	398	6000			
65°	50	84	1016	1016	89		7
80°		56	420				
100°		52	401	1000	2012	50	7

A self-supporting aluminium target of 170 μg/cm^2 thickness was bombarded by the internal proton beam of COSY. Three beam energies were used: 1.2, 1.9, and 2.5 GeV. To assure the same experimental conditions for all beam energies COSY operated in the so-called supercycle mode. In this mode several cycles were alternated for each requested beam energy, consisting of protons being injected from the cyclotron JULIC to the COSY ring, their acceleration with the beam circulating in the ring below the target, and irradiating the target by slow movement of the beam in the upward direction. Due to the application of the supercycle mode of the target irradiation, all conditions of the experiment except the energy of the proton beam remained unchanged. This allowed us to minimize the effect of systematic uncertainties on the projectile energy dependence of the measured cross sections. The $d^2\sigma/d\Omega\, dE$ were measured for the following ejectiles: p, d, t, ^{3,4,6}He, ^{6,7,8,9}Li, ^{7,9,10}Be, ^{10,11}B, and C.

In order to allow for absolute normalization of differential cross sections, we performed a "two moving sources" fit to $d^2\sigma/d\Omega\, dE$ for ^{7}Be production in our experiment, and compared the resulting total cross section with the data from Ref. [21]. It was found that the angular and energy dependence of $d^2\sigma/d\Omega\, dE$ can be well reproduced by a

simple formula representing the isotropic emission from two sources moving forward along the beam direction. Each source emitting particles with Maxwellian energy distribution was characterized by its velocity β, temperature T, height of the Coulomb barrier between ^{7}Be and the source remnant described by parameter k, and by emission intensity σ (see the Appendix of Ref. [1] for details of the parametrization). The σ parameter has the meaning of the energy and angle-integrated cross section attributed to a given source. Thus, the non-normalized cross section $\sigma_{\text{a.u.}}$ for ^{7}Be production is equal to the sum of parameters $\sigma_1 + \sigma_2$ for both sources. Best values of the parameters were found by fitting simultaneously the full set of the ^{7}Be spectra (seven scattering angles). Unfortunately, the fits lead to ambiguous results because the experimental spectra did not cover the full energy range allowed by kinematics. Low-energy particles were not registered because of finite low-energy detection thresholds of the telescopes. This lack of information on the low-energy part of spectra could strongly influence the value of the energy integrated cross section, since the spectra have Maxwellian shape with the maximum lying in the neighborhood of the energy threshold. Fortunately, it turned out that the spread of values of σ parameters was smaller than 10% among the sets of parameters which provided the same, best χ^2 values obtained for various combinations of fixed Coulomb barrier parameters k_1 and k_2. The final values of the σ parameters for both sources were taken as the arithmetic mean of results obtained for equivalent quality fits, i.e., those which have the same, smallest χ^2 value. The error of the normalization factor obtained in such a way was around 9% for all studied energies. It should be pointed out that such a procedure cannot guarantee that the total systematic error caused by lack of information on the low-energy part of the ^{7}Be spectra is taken into account. The above quoted error does not include the inaccuracy of the literature value of the production cross section $\sigma(^7\text{Be})$ [21], which is believed to be smaller than 10%.

The good quality of the absolute normalization of the present experiment is confirmed by a comparison of the obtained differential cross sections with the data from literature. To our knowledge only one measurement of light charged particle spectra as well as intermediate mass fragment spectra is present in the literature for an aluminium target at proton beam energies similar to those used in the present study. This is the paper of Westfall *et al.* [9] dealing with reactions in the p + Al system investigated at 4.9 GeV proton energy. This energy is 2–4 times higher than those used in the present work; however, it is known that the total production cross sections for this target vary only slightly at proton beam energies larger than 1 GeV (cf., e.g., Ref. [21]). As is also shown in [21], in contrast to heavier targets this limiting fragmentation occurs for the p + Al system already at approximately 1 GeV. The differential cross sections measured in the present experiment also change only slightly with the beam energy, as is shown in Fig. 1 for p, d, and t and in Fig. 2 for ^{4}He, ^{7}Li, ^{9}B, and ^{11}B. As can be seen, the cross sections increase very slightly with the increasing beam energy. This increase is stronger for lighter ejectiles ($p, d, t, ^4$He, ^{7}Li), whereas the data for heavier IMFs are in the limits of errors, independent of the beam energy.

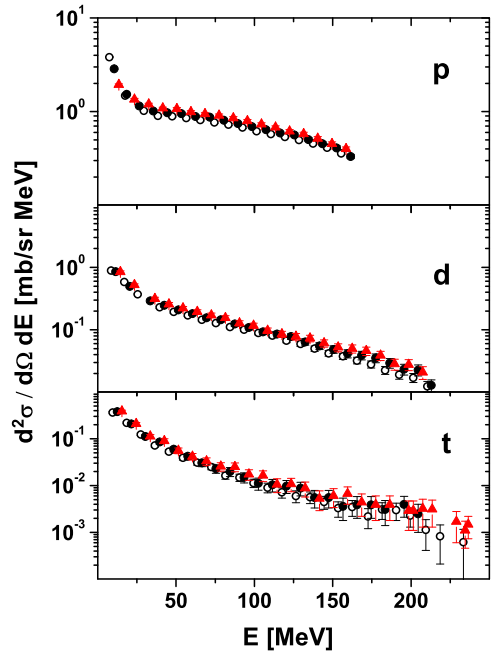

FIG. 1. (Color online) Spectra of p, d, and t measured at 65° for p + Al collisions at three proton beam energies: 1.2 (circles), 1.9 (dots), and 2.5 GeV (triangles). To avoid overlapping of symbols only different energy bins are shown for different beam energies.

The weak energy dependence of the differential cross sections leads to the conclusion, that it is reasonable to compare the present data with the results obtained by Westfall *et al.* [9] at even higher incident proton energy. Such a comparison is depicted in Fig. 3 for lithium, beryllium, and boron isotopes.

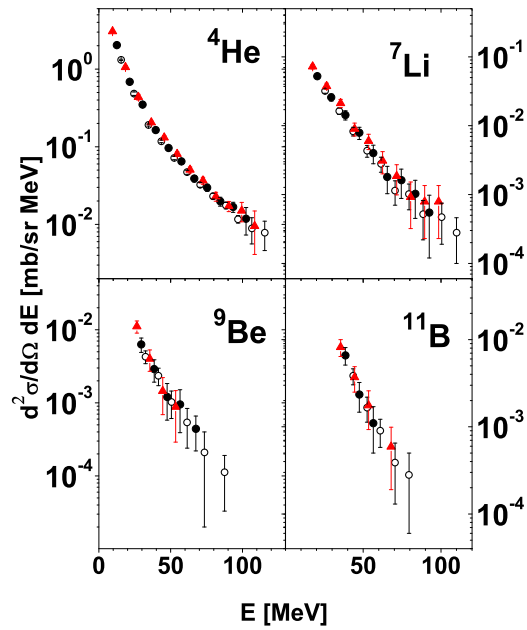

FIG. 2. (Color online) Same as Fig. 1, but for ^{4}He, ^{7}Li, ^{9}Be, and ^{11}B measured at 35°.

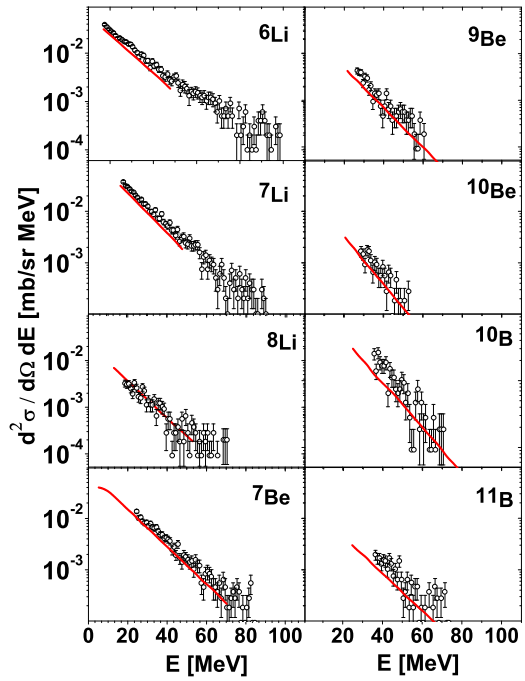

FIG. 3. (Color online) Experimental spectra of Li, Be, and B from the present work (circles) measured at 100° in p + Al collisions at proton beam energy 2.5 GeV, and data from Ref. [9] measured at 90° at proton energy 4.9 GeV (lines).

As can be seen, the shapes and magnitudes of the spectra are in good agreement for all ejectiles.

III. THEORETICAL ANALYSIS

The model calculations of the first stage of the reaction were done by means of the commonly used INCL4.6 computer program [14,22,23] realizing the intranuclear cascade of nucleon-nucleon collisions. The decay of remnant nuclei (A,Z) excited to the energy E^* was evaluated in the frame of three different models: the evaporation/fission model ABLA07 of Kelić *et al.* [15], the statistical multifragmentation model SMM of Botvina *et al.* [16], and the sequential binary decay model GEMINI++ of Charity [17]. These models are briefly described in the following subsection. In the second subsection the comparison of data with the results of the models is presented.

A. The description of the theoretical models

The INCL4.6 approach [14] resembles to a large extent the semiclassical microscopic description of a collision between a particle and a nucleus. As for any intranuclear cascade model, the basic physical assumptions apply also for the INCL model. The motion of nucleons between collisions proceeds in the square potential well whose radius depends on the nucleon momentum. The depth of the potential well felt by the nucleons is dependent on the energy of the nucleons according to the phenomenology of the real part of the optical-model potential. Furthermore, it is different for protons and neutrons—adjusted in such a way as to assure equality of the energy of the neutron and proton Fermi levels. The nucleons move along straight lines until they undergo a collision with another nucleon or until they reach the surface. Then they escape if their total energy is positive and (for protons) if they manage to penetrate the Coulomb barrier. The charged particle trajectories entering or leaving the nucleus are deflected in the Coulomb field. The collisions of pairs of nucleons take place as instantaneous, point interactions with the cross sections of free nucleon-nucleon collisions. The quantum effects enter into the reaction by introducing Pauli blocking, which inhibits collisions leading to occupied states. The inelastic nucleon-nucleon collisions which are responsible for excitation of the delta-resonance and for emission of pions are taken into account. The average potential for pions is introduced as well as reflection and/or transmission at the border of this potential.

The characteristic property of the INCL4.6 model is a possibility to describe the emission of complex particles (with mass number $A \leqslant 8$) as clusters produced through a dynamical phase space coalescence model. The clusters with lifetime larger than 1 ms are treated as detectable. Those with shorter lifetime are forced to decay at the end of the cascade process. This property of INCL4.6 enables us to take into account the emission of complex particles in the first, fast stage of the reaction before the colliding proton-nucleus system achieves thermodynamic equilibrium.

Clearly, in the family of intranuclear cascade codes, the newest version of the INCL model appears to be the most sophisticated and elaborate code, including the latest hadron and meson reaction data and reaction mechanisms. The model was tested successfully against a large database; cf. Ref. [14] where a detailed description of the INCL4.6 model is reported.

It is assumed that the fast, cascade stage of the reaction is finished after approximately 10^{-22} s, leaving a thermalized residual nuclear system which is then deexcited by emission of nucleons and various complex particles according to several possible mechanisms. The three different models ABLA07, SMM, and GEMINI++, which were used in the present study to describe the deexcitation of the residual nuclei, are based on the following pictures of the process.

The ABLA07 code describes the deexcitation of the residual compound nucleus $(A_{\rm res}, Z_{\rm res})$ through evaporation of light particles, simultaneous breakup, and fission. If the excitation energy per nucleon of the residual nucleus $\varepsilon_{\rm res} \equiv E^*_{\rm res}/A_{\rm res}$ exceeds a limiting value $\varepsilon_{\rm freeze\text{-}out}$ (a default value of $\varepsilon_{\rm freeze\text{-}out} = 4.2$ MeV/nucleon is used), the nucleus undergoes breakup into several fragments, otherwise evaporation and/or fission processes appear. The evaporation process is realized according to the Weisskopf-Ewing formalism [24], which in its standard form does not involve the angular momentum and parity but calculates the probability of particle emission from the energy-dependent cross sections of inverse reactions, level densities of daughter nuclei, as well as Coulomb barriers for charged emitted particles. ABLA07 extends the Weisskopf-Ewing formalism by random sampling of the angular momentum change in the evaporation process from a Gaussian distribution with specifically chosen parameters. The model takes into consideration the realistic level densities, the Coulomb barriers which are especially important at small energies of emitted

particles, and the effect of thermal expansion of the excited nucleus.

The fission probability, which is negligibly small for such a light target as Al but is important for heavy targets, is determined from time-dependent approach, as described in Ref. [15] and papers cited therein.

At high excitations of the residual nucleus, i.e., $\varepsilon_{\rm res} > \varepsilon_{\rm freeze\text{-}out}$, the breakup process of the nucleus is involved. The calculation of the yields of emitted particles is performed according to the following reasoning: It is assumed that the excess of the excitation energy per nucleon $\varepsilon_{\rm res}$ of the residual nucleus $(A_{\rm res}, Z_{\rm res})$ over the critical value $\varepsilon_{\rm freeze\text{-}out}$ is spent for the creation of a lighter residual nucleus $(A_{\rm freeze\text{-}out}, Z_{\rm freeze\text{-}out})$ accompanied by nucleons and light fragments. Since conservation of the A/Z ratio is postulated, the knowledge of $\varepsilon_{\rm res}$ and $\varepsilon_{\rm freeze\text{-}out}$ enables determining $A_{\rm freeze\text{-}out}$ as well as $Z_{\rm freeze\text{-}out}$ of the final residual nucleus and its excitation energy if the energy spent in losing one mass unit is fixed. This energy is estimated from experimental studies of the ^{238}U + Pb reaction at 1 A GeV [25] and it varies from 10 MeV for initial excitation energy 2.9 A MeV to 5 MeV for 11.8 A MeV initial excitation energy. The mass numbers of light particles are sampled from the exponential distribution

$$\frac{d\sigma}{dA} \propto A^{-\tau(E^*/A)},$$

where a linear dependence of τ on the E^*/A is assumed. The atomic number of fragments is sampled from a Gaussian distribution centered around a value imposed by conservation of the A/Z ratio with the standard deviation determined by the temperature at the freeze-out point. The kinetic energy spectra of fragments are evaluated in two different pictures of the breakup; if the timescale of the process is short for thermal equilibration to establish, the decay is governed by the Fermi motion of nucleons in the breakup system, whereas for the long-timescale process the thermal motion of fragments inside the breakup volume plays a decisive role. Each of the break-up fragments greater than an α particle is a subject to deexcitation via the evaporation cascade. Further details of the ABLA07 model as well as values of its parameters may be found in Ref. [15].

The statistical multifragmentation model (SMM), which was developed by Botvina *et al.* [26–28], assumes that the thermalized residual nucleus of the first stage of the proton-nucleus collision undergoes a statistical breakup. At first the nucleus expands to a certain volume and then breaks up into nucleons and hot fragments. All possible breakup channels are considered. The probability w_j of a specific decay channel j of the nucleus excited to the energy E^* is proportional to the exponential function of the entropy $S_j(E^*)$, which (besides the excitation energy) depends also on other parameters of the system:

$$w_j \propto \exp[S_j(E^*)].$$

The model treats the formation of a compound nucleus as one of the decay channels. This allows for the transition from evaporation at low energies to multifragmentation at high excitations on the basis of the available phase space. It is assumed that at the breakup time the nucleus is in thermal equilibrium characterized by the channel temperature T. The light fragments with mass number $A \leqslant 4$ and atomic number $Z \leqslant 2$ are treated as structureless particles, i.e., they have only translational degrees of freedom. The heavier fragments are considered as heated drops of nuclear liquid, thus their individual free energies are parametrized according to the liquid-drop model, i.e., they are equal to sum of the bulk, surface, Coulomb, and symmetry energies. The Coulomb interaction between all fragments is taken into account via the Wigner-Seitz approximation. The breakup channels are simulated by the Monte Carlo method according to their statistical weights. After breakup of the system, the fragments propagate independently in their mutual Coulomb fields and undergo secondary decays. The de-excitation of large fragments (with mass number larger than 16) is described by the evaporation-fission model whereas that of smaller fragments by the Fermi breakup model. A detailed description of the model and its parameters is provided by Ref. [16].

The GEMINI++ is a Monte Carlo code which describes the decay of compound nucleus by a series of binary divisions until the resulting products are unable to undergo further decay [17]. The GEMINI code was originally created by R. J. Charity to account for complex-fragment formation in heavy-ion fusion experiments [18]. Since heavy-ion reactions involve large values of the angular momentum, the treatment of the spin and orbital angular momentum in the deexcitation of the compound nucleus should be as exact as possible. For this reason the Hauser-Feshbach formalism which explicitly treats and conserves angular momentum was used to describe evaporation of light particles (with Z up to 4) instead of the simpler Weisskopf-Ewing formalism which neglects spin effects. The partial decay widths for more symmetric divisions of the compound nucleus were taken from Moretto's generalized transition-state formalism. Whereas this method provides an adequate description of the decay of light compound nuclei, it is not accurate enough for heavier nuclei. An improved version of the code, GEMINI++, was made to overcome this problem [17,29]. In this code the Bohr-Wheeler formalism is used for symmetric fission, and the width of the mass distributions of the fission fragments is interpolated from systematics. However, the Moretto formalism is kept for both light systems and for asymmetric divisions of heavy systems. It should be emphasized that in GEMINI++ an effort was made to systematize parameters which provide a good overall agreement with light particle evaporation data from a large range of compound-nucleus masses [30]. However, this optimization was only done for the regions of spin and excitation energies populated by heavy ion fusion reactions, which may not coincide with those produced in spallation.

The three models of the second stage of the reaction discussed above have been used together with INCL4.6 by Boudard *et al.* [14] for the description of proton-induced reactions in a broad range of proton energies and target masses. ABLA07 and SMM explicitly take into account a possibility of multifragmentation of the excited remnant of the first stage of the reaction. GEMINI++, on the other hand, treats the deexcitation of this remnant as a series of binary decays. In the present study the standard values of the parameters have been kept as in Ref. [14] without an attempt to make any fit to the

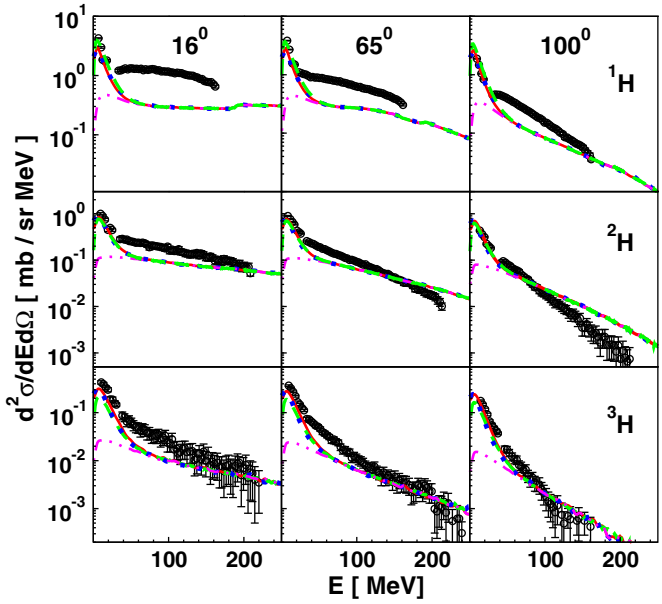

FIG. 4. (Color online) Experimental spectra (circles) for p + Al collisions at proton beam energy of 1.2 GeV measured at three scattering angles: 16°, 65°, and 100° (left, middle, and right columns) for protons, deuterons and tritons (upper, middle, and lower rows). The lines represent theoretical calculations. The magenta (dotted-dashed) line represents calculations performed by INCL4.6 model with inclusion of coalescence whereas the green (dashed), red (solid), and blue (dotted) lines correspond to the sum of INCL4.6 calculations with ABLA07, SMM, and GEMINI++ contributions, respectively.

experimental data. This allows us to observe predictive power of the theoretical models involved.

B. Comparison of the data with theoretical models

The quality of the description of experimental data for p + Al collisions may be judged from inspection of Figs. 4–8, where a representative sample of the data measured at proton beam energy equal to 1.2 GeV is shown. As it was discussed in the previous section of this paper, the experimental cross sections almost do not change in the studied energy range. This concerns both the magnitude of the cross sections as well as the shape of angular and energy dependence of $d\sigma/d\Omega\, dE$. This property of the data is well reproduced by all applied models; i.e., also the theoretical cross sections almost do not vary in the studied beam energy range from 1.2 to 2.5 GeV. It is worthy of note that Figs. 4–8 are representative of the quality of data reproduction obtained at all studied energies due to the above features of the data and the model cross sections.

Another qualitative property of the data—the presence of two components of the spectra: the quasisotropic low-energy component and the forward peaked high-energy contribution—is also reproduced by the applied models. Moreover, all the models assign the high-energy contribution to the first stage of the reaction and the low-energy component to the emission of nucleons and composite particles from the excited-nucleus remnant of the first step of the reaction.

The quantitative agreement between the data and the theoretical cross sections is varying with the type of ejectiles and with applied models. The cross sections evaluated by INCL4.6+ABLA07, INCL4.6+SMM, and by INCL4.6+GEMINI++ are depicted in Figs. 4–8 by dashed (green), solid (red), and dotted (blue) lines, respectively. The contribution of the INCL4.6 is shown as a double dotted-dashed (magenta) line. It should be emphasized that the fluctuations of the theoretical curves visible in the figures have no meaning; they are only due to a limited statistics of the Monte Carlo calculations. In the following we will discuss separately the quality of reproduction of the data for individual elements.

The hydrogen spectra which are shown in Fig. 4 contain the proton (upper row of the figure), the deuteron (the middle row), and the triton (the lowest row) data measured at a proton beam energy of 1.2 GeV. The experimental as well as the theoretical spectra show different angular dependences for small ejectile energies (up to about 30 MeV) and for higher energies. The cross sections in the low-energy region depict Maxwell-like, angle independent energy dependence, whereas they behave in a different manner in the higher energy region. There they decrease exponentially with the energy for all angles, but the slope of this exponential function is angle dependent: it monotonically increases with the emission angle. All three theoretical models show that the low-energy region in the spectra is dominated by the emission of particles from the second stage of the proton-nucleus collisions, i.e., from the excited remnant of the intranuclear cascade of nucleon-nucleon collisions. The best description of the low-energy proton spectra seems to be offered by ABLA07, whereas such spectra for deuterons and tritons are reproduced in the best way by the SMM model. The high-energy tail of the spectra is not populated in the second stage of the reaction. On the contrary, it is dominated by the emission of particles from the first, nonequilibrium stage of the proton-nucleus collisions. In the case of proton emission this part of the spectra originates (naturally) from the nucleon-nucleon cascade of collisions. High-energy deuterons and tritons are also emitted from this fast stage of the collisions but they appear only due to the effect of coalescence.

The most striking evidence inferred from Fig. 4 is strong underestimation of the high-energy part (from about 40 to about 150 MeV) of the proton spectra by the theoretical model. The difference between the experimental cross sections and the calculated ones diminishes with the scattering angle, but even for 100° the former cross sections are about factor of 2 larger than the latter. The maximal difference is placed around 100 MeV energy of ejectiles. The same qualitative but much smaller difference between experimental and calculated cross sections is visible for deuterons and for tritons. Another difference consists of the faster increase of the slope of the experimental spectra with increased scattering angle than the increase of the slope of the theoretical spectra. A similar effect has been observed for reactions induced by GeV protons on Ni and Au targets [2–4]. For these heavier targets the analogous effect was energy dependent, i.e., it was most pronounced at the highest beam energy. Since the experimental and theoretical spectra for the Al target are almost independent

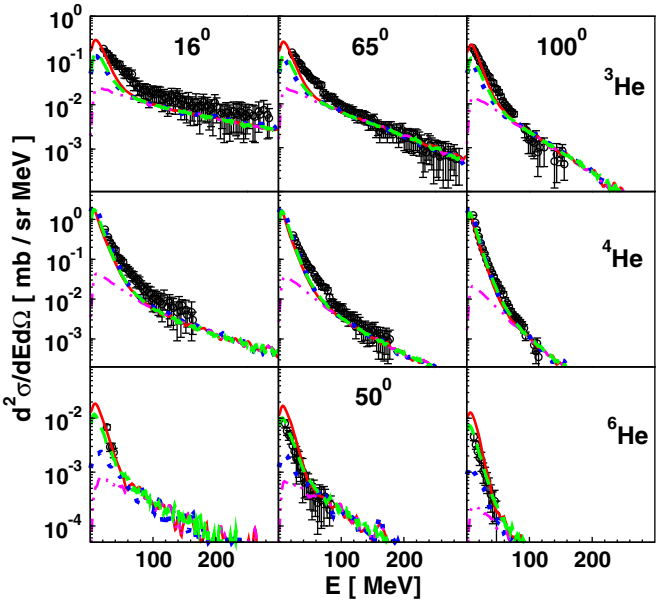

FIG. 5. (Color online) Same as in Fig. 4 but for ^{3}He, ^{4}He, and ^{6}He, respectively.

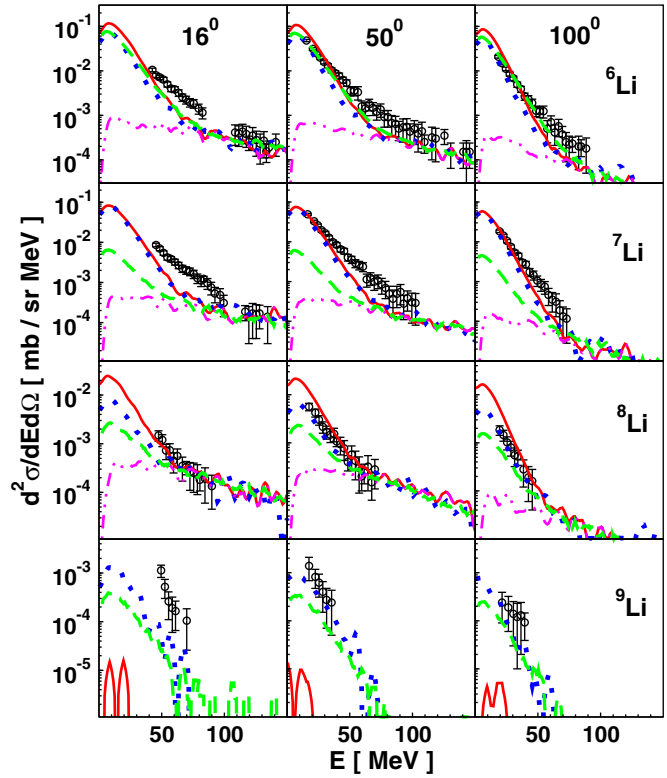

FIG. 6. (Color online) Same as in Fig. 4 but for ^{6}Li, ^{7}Li, ^{8}Li and ^{9}Li, respectively. Note that there is no contribution of the coalescence process for ^{9}Li spectra because the mass number for coalescence is limited to 8 in the INCL model currently.

of the beam energy, this effect cannot be observed in the present investigations.

The helium spectra are presented in Fig. 5. In the top row of the figure the ^{3}He, in the middle the ^{4}He, and in the bottom row the ^{6}He data are compared with model cross sections. The behavior of the spectra for ^{3}He and ^{4}He is similar to that of the deuteron and triton data. The spectra for energies higher than about 50 MeV are dominated by the coalescence process which reproduces the experimental spectra for energies higher than about 100 MeV. On the other hand, the low-energy part of the spectra is dominated by processes of emission of particles from the second stage of the reaction. All the models, ABLA07,GEMINI++, and SMM, predict the same behavior of the α particle cross sections, however, the agreement with the data is good only at very low energies (smaller than about 20 MeV). Similarly to hydrogen isotopes, there exists a significant difference (factor 2) between the data and theoretical cross sections for the α particle energies in the range from about 30 to about 80 MeV. The underestimation of the ^{3}He data in this energy range by the model cross sections is even larger. Furthermore, the SMM provides for ^{3}He the best agreement with the data, whereas both other models give very similar results but the agreement with the data is poorer. A different situation is present for ^{6}He where ABLA07 gives the best agreement with the data, SMM describes them quite reasonable, but GEMINI++ predicts cross sections significantly smaller (at energies smaller than about 40 MeV) than the data. The spectra at higher energies are dominated by the coalescence process. The agreement is satisfactory within the range of energies where data are available (smaller than about 80 MeV).

It seems that the character of deviations of the model spectra from the data is the same for ^{3}He and for ^{4}He as that for hydrogen isotopes. Furthermore, the agreement improves generally with increasing ejectile mass. This is true for the full range of the energies but is especially pronounced for energies above 100 MeV, where the coalescence process is fully responsible for the theoretical cross sections. Such a conclusion cannot be made for ^{6}He because of the lack of the data in the corresponding range of energies.

As shown in Fig. 6, the experimental spectra of all lithium particles, i.e., ^{6}Li, ^{7}Li, ^{8}Li, and ^{9}Li have very similar shapes, but the absolute yield of ^{8}Li decreases by one order of magnitude and that of ^{9}Li by almost two orders of magnitude with respect to ^{6}Li and ^{7}Li cross sections. GEMINI++ and SMM reproduce well such an isotopic dependence of the reaction yield; however, the SMM strongly underestimates (by two orders of magnitude) the ^{9}Li cross sections. ABLA07 describes well spectra of ^{6}Li but underestimates cross sections for heavier lithium isotopes. It should be also noted, that the coalescence contribution was not calculated for ^{9}Li because the INCL4.6 limits at present such calculations to particles with mass number smaller than 9. From inspection of Fig. 6 it seems that the cross sections predicted by coalescence models decrease slowly with increasing mass of lithium particles: they decrease only by factor of 2–3 from ^{6}Li to ^{8}Li. It is therefore quite likely that adding the coalescence effect to the ^{9}Li spectra may significantly improve the theoretical description of these data.

All the models reproduce the shape of the experimental spectra for Be and B isotopes as depicted in Figs. 7 and 8, with slightly larger slopes of the exponential decrease with energy than shown the data. This effect may be caused by

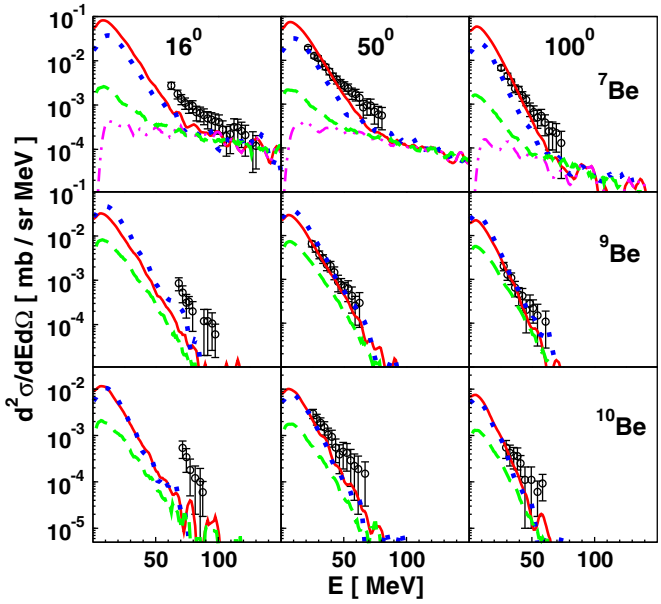

FIG. 7. (Color online) Same as in Fig. 4 but for ^{7}Be, ^{9}Be, and ^{10}Be, respectively. The coalescence contribution was not included for two heavier Be isotopes because their mass number is larger than 8.

INCL4.6 neglecting the coalescence contribution for particles with mass number larger than 8. Such a conclusion may be supported by the fact that the largest disagreement is observed always for the spectra measured at 16°, where the experimental data were measured for larger energies (around 100 MeV), i.e., such energies where the exponentially falling spectra predicted by processes of emission from the excited remnant of the cascade give negligible contribution. In this energy range the coalescence contribution which is almost energy independent may start to dominate, as is visible in the case of the ^{7}Be spectra shown in the upper row of Fig. 7. It is evident that the description of the ^{7}Be spectrum measured at 16° would be much poorer without inclusion of the coalescence process. The GEMINI++ and SMM models describe well the experimental cross sections for ^{7}Be, ^{9}Be, and ^{10}Be; however,

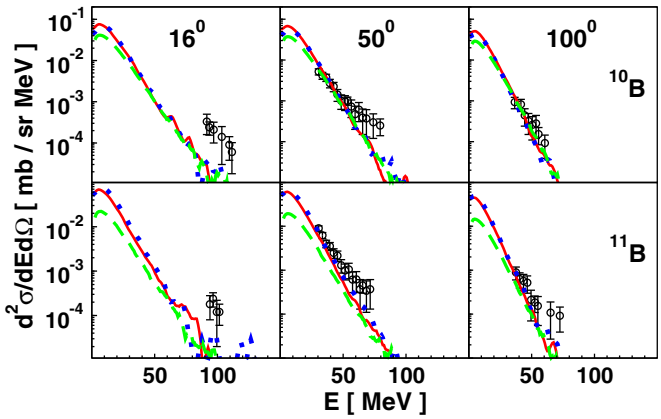

FIG. 8. (Color online) Same as in Fig. 4 but for ^{10}B and ^{11}B, respectively. The coalescence contribution was not included because the mass number of both these fragments is larger than 8.

ABLA07 underestimates the magnitude of all Be spectra. For ^{10}B and ^{11}B spectra all the models reproduce the experimental cross sections, showing, however, a need to introduce another (e.g., coalescence) contribution for energies larger than about 60 MeV.

IV. SUMMARY AND CONCLUSIONS

In the present work an experiment was performed with the aim to measure the double differential cross sections $d^2\sigma/d\Omega dE$ for light charged particles and intermediate mass fragments produced in p + Al collisions at three proton energies: $T_p = 1.2$, 1.9 and 2.5 GeV. The spectra of protons, deuterons, tritons, ^{3,4,6}He, ^{6,7,8,9}Li, ^{7,9,10}Be, and ^{10,11}B were measured at seven scattering angles from 15.6° to 100°. To our knowledge it is the only such set of cross sections measured for an Al target in this energy range. The shapes of the experimental spectra as well as their angular dependence resemble to a large extent results obtained earlier in this beam energy range for heavier targets: Au [1,2] and Ni [3,4]. The energy dependence of the absolute value of the cross sections is very weak, in contrast to that observed for heavier targets in this energy range. It can be stated that the variation of the absolute cross section is the largest for Au which is the heaviest target, smaller for the intermediate mass Ni target, and practically vanishes (at least for heavier products) for the lightest Al target. It is in agreement with previous findings that the leveling of the total production cross sections appears at lower beam energies for light targets than for heavy ones (cf., for example, [21]).

The measured data were confronted with theoretical calculations performed by means of the INCL4.6 computer program, which describes the fast stage of proton-nucleus collisions as an intranuclear cascade of nucleon-nucleon and nucleon-pion collisions, allowing not only for emission of the nucleons but also emission of complex particles. This is realized assuming that complex particles are formed by the coalescence process. It was found that such a contribution is necessary for the description of the high-energy part of the spectra for light charged particles as well as for intermediate mass fragments.

The nuclei-excited remnants of the first stage of the reaction were allowed to emit particles due to both evaporation as well as multifragmentation processes. To take all possible processes into consideration, three different models were applied for the description of the second stage of the reaction: ABLA07, GEMINI++, and SMM. Each of these models takes into account different scenarios of deexcitation of the thermalized remnant nucleus. Our calculations were parameter free, i.e., the standard parameters recommended by authors of the models were used. It was found that all three models coupled with the INCL4.6 describe in very similar manner the emission of light charged particles, as well as emission of ^{6}Li, ^{10}B, and ^{11}B. The GEMINI++ and SMM models produce also very similar spectra for ^{7}Li and for three isotopes of Be, i.e., ^{7}Be, ^{9}Be, and ^{10}Be. The cross sections evaluated by ABLA07 for these isotopes are significantly smaller. The largest deviations between predictions of different models appear for ^{6}He and for ^{9}Li, where the data are strongly underestimated by GEMINI++ and SMM, respectively.

The largest disagreement of the measured cross sections and those calculated by all the models is present for protons (the data are even about 5 times higher than the theoretical spectrum at 16°) and it gradually decreases with increasing mass of the emitted particle. Such an effect suggests that an important mechanism of the particle emission is missed in the theoretical description of the reactions. Similar underestimation of the experimental cross sections of light charged particles emission by theoretical models for the energy range between about 30 and ∼150 MeV was observed in the previous studies of proton-induced reactions on Ni [3,4] and Au [1,2] targets. It was shown that the energy and angular dependence of this lacking cross section can be reproduced by the emission of particles from a fast, hot source moving in the forward direction. The present observation together with the above mentioned findings calls for development of the theoretical models of the fast stage of the proton-induced reactions at GeV energies.

It is interesting to note that the cross sections for the emission of neutrons [31] from proton-induced reactions on the Al target at the same beam energy, 1.2 GeV, as that used in the present experiment agree much better with theoretical predictions than our proton data. Such a significant difference between the behavior of proton and neutron cross sections was not observed for heavier targets, i.e., for Ni [3,4] and Fe [31] as well as for Au [1,2] and Pb [31]. The origin of this effect is not clear. It is, however, important to take into consideration that the disagreement of the theoretical proton cross sections with the data may influence also the quality of the reproduction of the high-energy tail of the IMF spectra, where the coalescence of the nucleons plays a crucial role.

ACKNOWLEDGMENTS

The technical support of A. Heczko, W. Migdał, and N. Paul in preparation of experimental apparatus is greatly appreciated. This work was supported by the European Commission through European Community–Research Infrastructure Activity under FP6 project Hadron Physics (Contract No. RII3-CT-2004-506078), and HadronPhysics2 (Contract No. 227431). We thank the code developers and authors A. Boudard, J. Cugnon, J. C. David, S. Leray, and D. Mancusi for providing us the latest version of their Liege intranuclear cascade code INCL4.6. We are also grateful A. Kelić-Heil for the improved version of ABLA07. One of us (S.K.S) acknowledges gratefully the support by the Foundation for Polish Science–MPD program, cofinanced by the European Union within the European Regional Development Fund.

[1] A. Bubak, A. Budzanowski, D. Filges, F. Goldenbaum, A. Heczko, H. Hodde, L. Jarczyk, B. Kamys, M. Kistryn, St. Kistryn, St. Kliczewski, A. Kowalczyk, E. Kozik, P. Kulessa, H. Machner, A. Magiera, W. Migdał, N. Paul, B. Piskor-Ignatowicz, M. Puchała, K. Pysz, Z. Rudy, R. Siudak, M. Wojciechowski, and P. Wüstner, Phys. Rev. C **76**, 014618 (2007).

[2] A. Budzanowski, M. Fidelus, D. Filges, F. Goldenbaum, H. Hodde, L. Jarczyk, B. Kamys, M. Kistryn, St. Kistryn, St. Kliczewski, A. Kowalczyk, E. Kozik, P. Kulessa, H. Machner, A. Magiera, B. Piskor-Ignatowicz, K. Pysz, Z. Rudy, R. Siudak, and M. Wojciechowski, Phys. Rev. C **78**, 024603 (2008).

[3] A. Budzanowski, M. Fidelus, D. Filges, F. Goldenbaum, H. Hodde, L. Jarczyk, B. Kamys, M. Kistryn, St. Kistryn, St. Kliczewski, A. Kowalczyk, E. Kozik, P. Kulessa, H. Machner, A. Magiera, B. Piskor-Ignatowicz, K. Pysz, Z. Rudy, R. Siudak, and M. Wojciechowski, Phys. Rev. C **80**, 054604 (2009).

[4] A. Budzanowski, M. Fidelus, D. Filges, F. Goldenbaum, H. Hodde, L. Jarczyk, B. Kamys, M. Kistryn, St. Kistryn, St. Kliczewski, A. Kowalczyk, E. Kozik, P. Kulessa, H. Machner, A. Magiera, B. Piskor-Ignatowicz, K. Pysz, Z. Rudy, R. Siudak, and M. Wojciechowski, Phys. Rev. C **82**, 034605 (2010).

[5] R. E. L. Green and R. G. Korteling, Phys. Rev. C **22**, 1594 (1980).

[6] R. E. L. Green, R. G. Korteling, J. M. DAuria, K. P. Jackson, and R. L. Helmer, Phys. Rev. C **35**, 1341 (1987).

[7] C.-M. Herbach, D. Hilscher, U. Jahnke, V. G. Tishchenko, J. Galin, A. Letourneau, A. Péghaire, D. Filges, F. Goldenbaum, L. Pieńkowski, W. U. Schröder, and J. Töke, Nucl. Phys. A **765**, 426 (2006).

[8] A. Letourneau, A. Böhm, J. Galin, B. Lott, A. Péghaire, M. Enke, C.-M. Herbach, D. Hilscher, U. Jahnke, V. Tishchenko *et al.*, Nucl. Phys. A **712**, 133 (2002).

[9] G. D. Westfall, R. G. Sextro, A. M. Poskanzer, A. M. Zebelman, G. W. Butler, and E. K. Hyde, Phys. Rev. C **17**, 1368 (1978).

[10] E. K. Hyde, G. W. Butler, and A. M. Poskanzer, Phys. Rev. C **4**, 1759 (1971).

[11] A. M. Poskanzer, G. W. Butler, and E. K. Hyde, Phys. Rev. C **3**, 882 (1971).

[12] J.-C. David, D. Filges, F. Gallmeier, M. Khandaker, A. Konobeyev, S. Leray, G. Mank, A. Mengoni, N. Otuka, and Y. Yariv, Prog. Nucl. Sci. Technol. **2**, 942 (2011).

[13] S. Leray, J. C. David, M. Khandaker, G. Mank, A. Mengoni, N. Otsuka, D. Filges, F. Gallmeier, A. Konobeyev, and R. Michel, J. Korean Phys. Soc. **59**, 791 (2011).

[14] A. Boudard, J. Cugnon, J. C. David, S. Leray, and D. Mancusi, Phys. Rev. C **87**, 014606 (2013).

[15] A. Kelić, M. V. Ricciardi, and K.-H. Schmid, in *Proceedings of the Joint ICTP-IAEA Advanced Workshop on Model Codes for Spallation Reactions, ICTP Trieste, Italy, 4–8 February 2008*, edited by D. Filges *et al.*, INDC(NDS)-530 (IAEA, Vienna, 2008), p. 181.

[16] J. P. Bondorf, A. S. Botvina, A. S. Iljinov, I. N. Mishustin, and K. Sneppen, Phys. Rep. **257**, 133 (1995).

[17] R. J. Charity, in *Proceedings of the Joint ICTP-IAEA Advanced Workshop on Model Codes for Spallation Reactions, ICTP Trieste, Italy, 4–8 February 2008*, edited by D. Filges *et al.*, INDC(NDS)-530 (IAEA, Vienna, 2008), p. 139.

[18] R. Charity, M. A. McMahan, G. J. Wozniak, R. J. McDonald, L. G. Moretto, D. G. Sarantites, L. G. Sobotka, G. Guarino, A. Pantaleo, L. Fiore *et al.*, Nucl. Phys. A **483**, 371 (1988).

[19] Z. Fraenkel, E. Piasetzky, and G. Kalbermann, Phys. Rev. C **26**, 1618 (1982).

[20] A. S. Fomichev, I. David, S. M. Lukyanov, Yu. E. Penionzhkevich, N. K. Skobelev, O. B. Tarasov, A. Matthies,

H.-G. Ortlepp, W. Wagner, M. Lewitowicz, M. G. Saint-Laurent, J. M. Corre, Z. Dlouhy, I. Pecina, and C. Borcea, Nucl. Instrum. Methods Phys. Res. A **344**, 378 (1994).

[21] A. Bubak, B. Kamys, M. Kistryn, and B. Piskor-Ignatowicz, Nucl. Instrum. Methods Phys. Res. B **226**, 507 (2004).

[22] A. Boudard, J. Cugnon, S. Leray, and C. Volant, Phys. Rev. C **66**, 044615 (2002).

[23] A. Boudard, J. Cugnon, S. Leray, and C. Volant, Nucl. Phys. A **740**, 195 (2004).

[24] V. F. Weisskopf and D. H. Ewing, Phys. Rev. **57**, 472 (1940); **57**, 935 (1940).

[25] T. Enqvist, J. Benlliure, F. Farget, K.-H. Schmidt, P. Armbruster, M. Bernas, L. Tassan-Got, A. Boudard, R. Legrain, C. Volant, C. Böckstiegel, M. de Jong, and J. P. Dufour, Nucl. Phys. A **658**, 47 (1999).

[26] A. S. Botvina, A. S. Iljinov, and I. N. Mishustin, Sov. J. Nucl. Phys. **42**, 712 (1985).

[27] A. S. Botvina, A. S. Iljinov, I. N. Mishustin, J. P. Bondorf, R. Donangelo, and K. Sneppen, Nucl. Phys. A **475**, 663 (1987).

[28] A. S. Botvina, A. S. Iljinov, and I. N. Mishustin, Nucl. Phys. A **507**, 649 (1990).

[29] D. Mancusi, R. J. Charity, and J. Cugnon, Phys. Rev. C **82**, 044610 (2010).

[30] R. J. Charity, Phys. Rev. C **82**, 014610 (2010).

[31] S. Leray, F. Borne, S. Crespin, J. Fréhaut, X. Ledoux, E. Martinez, Y. Patin, E. Petibon, P. Pras, A. Boudard, R. Legrain, Y. Terrien, F. Brochard, D. Drake, J. C. Duchazeaubeneix, J. M. Durand, S. I. Meigo, G. Milleret, D. M. Whittal, W. Wlazlo, D. Durand, C. Le Brun, F. R. Lecolley, J. F. Lecolley, F. Lefebvres, M. Louvel, C. Varignon, F. Hanappe, S. Ménard, L. Stuttge, and J. Thun, Phys. Rev. C **65**, 044621 (2002).